Control Issues in Automated Highway Systems

J.K. Hedrick, M. Tomizuka, and P. Varaiya

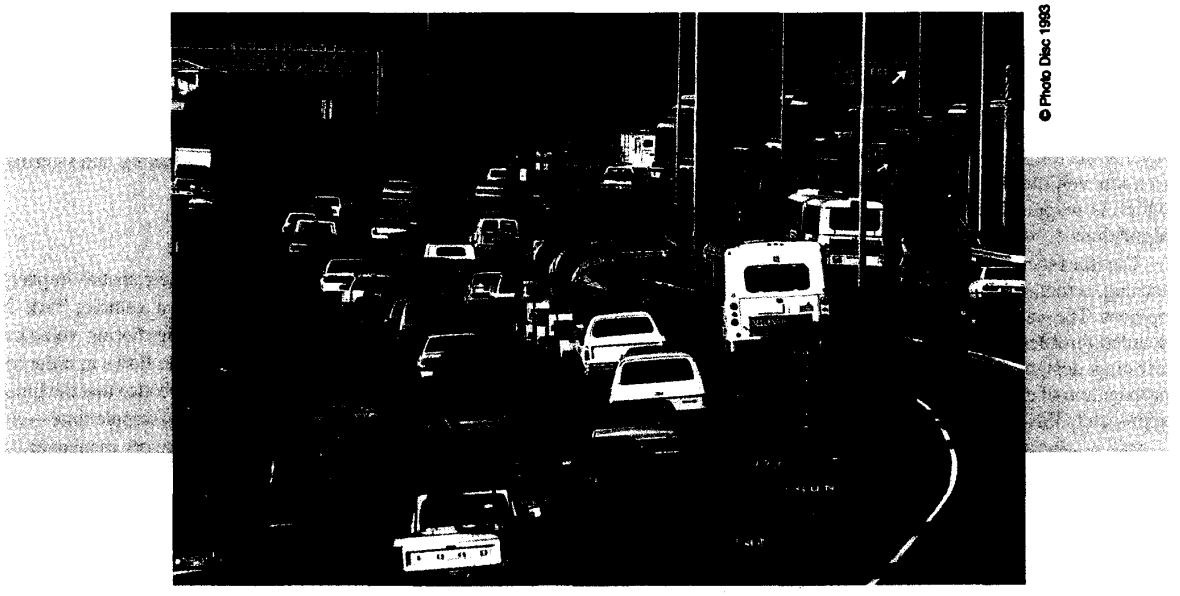

This article describes vehicle control issues that must be faced in designing a fully automated highway system (AHS). In particular, requirements for a control system architecture as well as issues of lateral and longitudinal "platoon" control are addressed. Interest in AHS is clearly expanding at a rapid pace due to the ever-increasing problems of freeway congestion and the potential for a technological solution. The approach described is based on five years of research as part of the California PATH program.

Introduction

The concept of an automated highway system is not a new one. An exhibit at the GM Pavilion of the 1939 World's Fair in New York aroused a good deal of interest. However, the problem, i.e., congestion, was not severe enough and the required technology was not mature enough to arouse more than a passing interest. Another surge of interest occurred in the early 1970s [1], when the newly created U.S. Department of Transportation tried to focus recent advances in aerospace technology on the ground transportation problem. Again, the seriousness of the congestion problem and the state of the art of control/communication/computer technology did not justify any widespread development programs. In this paper we will not provide a complete review of AHS history. Another paper in this issue, by R.E. Fenton, provides a more comprehensive review. A review paper by Shladover et al. [2] provides an overview of the Advanced Vehicle Control System (AVCS) research of the PATH program as of 1990. This paper will focus on the work accomplished since that review paper.

The principal motivation for an AHS is increased capacity. There have been many papers justifying this claim [2,3,4]. Essentially, the capacity (vehicles/lane/hour) can be increased by vehicles operating under automatic control at closer spacing than human drivers can operate. One can also argue that an AHS will be safer, since data suggest [4] that human error accounts for 90% of accidents. Estimates of the actual increase in capacity that an AHS would provide range from factors of 2 to 6 over current peak capacities (≈2000 vehicles/lane/hour). Varaiya [4] argues that a quadrupling of AHS capacity over existing peak flows is certainly feasible.

The second section of this paper discusses the requirements for a control system architecture. System level control is sepa-

The authors are with the University of California at Berkeley. *The research described in this paper was supported by the California PATH program. The authors would like to acknowledge the support of the many PATH research staff and UC Berkeley graduate students who have contributed to this research.*

 0272-1708/94/$04.00©1994IEEE

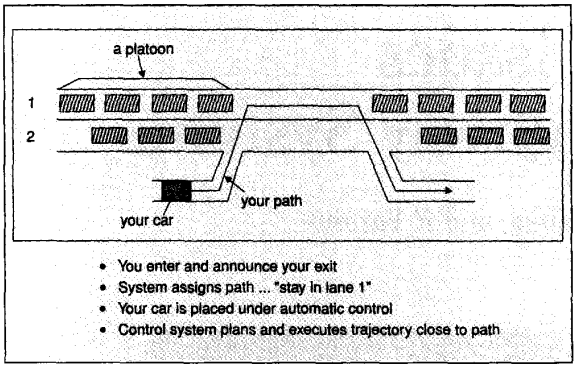

Fig. 1. AHS scenario.

rated into a multilayered architecture ranging from a network layer at the top level, which is responsible for assigning a route to each vehicle, down to a regulation layer at the bottom, which is responsible for throttle, brake, and steering control algorithms.

The third section discusses vehicle spacing control, including sensing, actuation, communication, and control algorithm development. The vehicle's longitudinal dynamics are modeled and detailed throttle/brake control algorithms are developed. An interesting design consideration for longitudinal control is the propagation of disturbances upstream in a string of vehicles. Our approach to this problem is presented.

The fourth section discusses lane-keeping control, including vehicle and road sensors, steering actuation requirements, and alternate steering control algorithms. The current PATH approach, i.e., permanent magnet discrete markers, is described, as well as its advantages over alternative technologies such as machine vision.

Control Structure

We begin by describing how a driver may experience the AHS, in order to determine the functions that the AHS control system must support. We then propose a control system structure that meets those goals.

AHS Control Tasks

To drive your car over a two-lane AHS, you enter from an on-ramp and announce your destination; see Fig. 1. Your vehicle's onboard computer communicates your destination to the roadside computer. It assigns you a lane (1 or 2) that you should occupy for most of your trip. Suppose it is Lane 1. It also tells your vehicle at what point along Lane 1 it should start changing lanes so that it can exit. We summarize these instructions by saying that the AHS assigns a *path* to your vehicle.[1] At some point on the entrance ramp, your car's computer takes over control. The computer will try to maintain a trajectory close to the assigned path. It begins by steering your car to change to Lane 2, and then to Lane 1. It will then keep your car in Lane 1 until you are close to your exit. It then changes lane again and enters the off-ramp. The computer then alerts you to take over control of the vehicle.[2]

A major objective of the AHS is to increase highway capacity and safety. This objective is achieved in part by organizing in platoons the traffic within each automated lane. A *platoon* is one or more vehicles traveling together as a group with relatively small spacing. Inter-platoon spacing is large. For example, with an average platoon size of 15, intra-platoon distance of 2 m, inter-platoon distance of 60 m, vehicle length of 5 m, and speed of 72 km/h, the maximum flow or capacity through an automated lane is more than over 6,000 vehicles/hour.[3]

In summary, there are three AHS control tasks:

1. To assign a path to each vehicle

2. To carry out safely the maneuvers of platoon formation, stabilization and dissolution, lane change, and entry and exit, and

3. To implement those maneuvers via feedback laws (algorithms) that control each vehicle's throttle, braking and steering actuators.

Proposed Control Structure

Observe how these three tasks vary in their spatial impact: Task 3 concerns the motion of an individual vehicle; Task 2 coordinates the movement of a group of neighboring vehicles affected by a maneuver; Task 1 adjusts vehicle flows in order to utilize efficiently a stretch of highway. Observe also that the time scales separate: Task 3 repeats at every control sample time—on the order of 30 ms; Task 2 is re-initiated with every maneuver—once a minute, on average; Task 1 calculations are repeated if there is a significant change in flow or if an incident occurs—every 10 minutes per km stretch of highway. Observe, finally, that the level of information detail needed to carry out these tasks varies: Task 3 requires information from vehicle sensors; Task 2 requires information about the movement of neighboring vehicles; Task 1 only requires aggregate speed and density of traffic flows in each lane.

Thus there is a clear separation among these tasks in terms of the range of spatial impact, the time scale, and the granularity of information. The control tasks must be organized within a structure that takes advantage of this separation. The proposed structure, depicted in Fig. 2, distributes the tasks in three control layers. At the bottom is the "plant"—the vehicle dynamics. The plant is directly controlled by the *regulation layer*. Above the regulation layer is the *coordination layer*. At the top is the *link layer*. We discuss each layer in more detail.[4]

[1] In an AHS with a network of highways, the vehicle would be assigned a *route* through the network, and a path along each highway in the route.

[2] Entry and exit are more complicated than suggested here. Entry includes procedures for "check-in" and for coordinating merging into Lane 2. Exit includes procedures for "check-out" and for control of the exiting vehicle in case its driver fails to resume control. See [5].

[3] The capacity is proportional to the speed. It is reduced if on- and off-ramps are closely spaced; see [6]. In addition to capacity benefits, some safety considerations favor a platoon organization [7].

[4] The distribution of equipment between private vehicles and public infrastructure is an important consideration of public policy. For the proposed control structure, it is natural to locate the regulation and control layers in computers onboard the vehicle, and the link layer on roadside computers. Earlier AHS proposals relied more heavily upon public infrastructure [8].

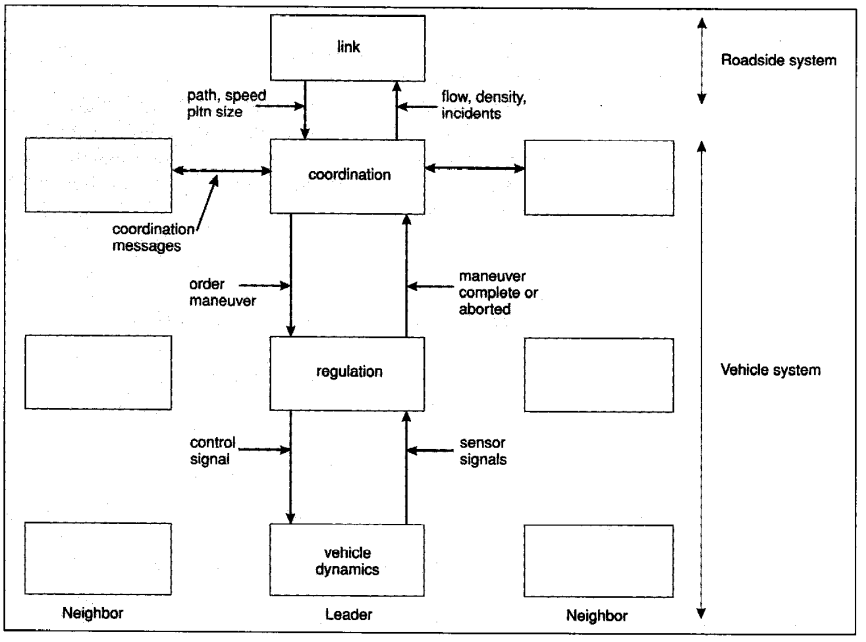

Fig. 2. AHS control structure.

Link Layer

The link layer broadcasts, for each 1 or 2 km stretch of highway, or *link*, target values for speed and platoon size for vehicles on that link, based on information about the aggregate traffic state (speed, density, flow). Using, in addition, estimates of the proportion of the traffic flow destined for the various exits, the link layer also advises vehicles where to begin changing lanes in order to reach their exits. It also receives information about incidents or congestion in downstream links. Based on that information, it may reassign vehicle paths. A link layer design is proposed and evaluated in [9].

Coordination Layer

Each vehicle's coordination layer determines which maneuver to initiate at any time so that it will conform to its assigned path; coordinates that maneuver with neighboring vehicles so that the maneuver can be undertaken safely; and then commands the regulation layer to execute the (pre-computed) feedback law that implements that maneuver. After some time, the regulation layer reports to the coordination layer that the maneuver is completed or aborted for reasons not anticipated by the coordination layer. Three maneuvers are proposed in [10]: join (which permits a platoon to join the platoon ahead of it); split (which separates a platoon into two); and lane change (which permits a one-car platoon to change lane).[5]

Each maneuver is coordinated by a structured exchange of messages—a protocol—among relevant neighboring vehicles. For example, "join" involves communication between the requesting platoon and the responding platoon ahead of it. A protocol is specified by a set of communicating finite state machines—one per vehicle involved in the protocol. This is similar to control protocols used in data communication networks. The specification is then checked for logical correctness. This requires affirmative answers to questions like "Does every request eventually get a proper response?" The design of [10] ends up with an overall state machine with 500,000 states. COSPAN [11] is used to prove correctness of the design. Seven feedback laws are necessary to implement the maneuvers:

1. Lead vehicle tracking: When not engaged in a maneuver, the lead vehicle must track the target speed (received by the link layer) and maintain a safe spacing from the platoon ahead.
2. Follower: A vehicle within a platoon that is not the lead must maintain a close spacing with the vehicle in front of it and keep within its lane.
3. Join: The lead vehicle must accelerate and then decelerate so that it joins the platoon ahead.
4. Split: A follower within a platoon must decelerate (so that a new platoon is formed) and then become a lead vehicle.
5. Lane change: A single vehicle must change to an adjacent lane.
6. Entry: A vehicle must enter the AHS from an on-ramp.
7. Exit: A vehicle must enter an off-ramp from the AHS.

Within PATH extensive research, including experimental testing, has been carried out for the "follower" law. That work is reviewed in the third and fourth sections of this paper.

Investigation of the other laws has been primarily limited to theoretical study and simulation. A major effort has gone into developing an AHS simulator called SmartPath [12]. SmartPath is a microsimulator in which the regulation, coordination, and link layer controllers are specified in a modular fashion. There are facilities for configuring the highway network, and for specifying traffic patterns. There is also a facility that gives a three-dimensional animation of the simulation results.[6]

The implementation of the system structure proposed places requirements on communication infrastructure, onboard computing and control, sensors, and actuators.

Spacing Control

Automated longitudinal control of a string of vehicles has received attention since at least the 1960s [13], and papers have appeared on the topics over the years since [14,15,16]. A very basic initial choice is to choose between a vehicle-follower and a point-follower approach. Reference [2] describes the PATH decision to develop a "platoon/vehicle-follower" approach. Pla-

[5]Maneuvers for entry and exit are proposed in [5].

[6]SmartPath is distributed by PATH. For information, write to delnaz@eclair.eecs.berkeley.edu.

tooning implies that the vehicles within a given platoon are very closely spaced, while the inter-platoon spacing is sufficiently large to allow emergency stopping. The tight spacing within the platoon allows the improvements in capacity as well as low-relative-velocity collisions in case of accidents [2]. The lead vehicle in the platoon will receive a target speed from the "link" layer while maintaining a safe headway (≈60 m) from the platoon in front of it [4]. This section will concentrate on vehicle-follower control algorithms for all the trailing vehicles within a platoon.

Longitudinal Vehicle Model

Fig. 3 shows a schematic of a vehicle's powertrain. Reference [17] develops a low-order nonlinear dynamic model that we will summarize here. The control inputs are the commanded throttle position and desired brake torque. The system output is the longitudinal acceleration and its integrals, velocity and position. Reference [17] shows that a nonlinear model is necessary to be accurate over a wide range of vehicle speeds, gear ratios, and throttle position. A variety of longitudinal models have been developed by the PATH program. Reference [18] describes these models in detail. Reference [19] describes a more detailed engine model from which the model in [18] is based. A simplified model for control system design can be formulated by making the following assumptions:

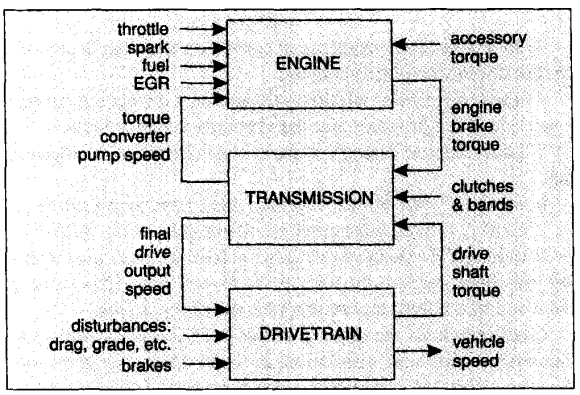

Fig. 3a. Vehicle powertrain.

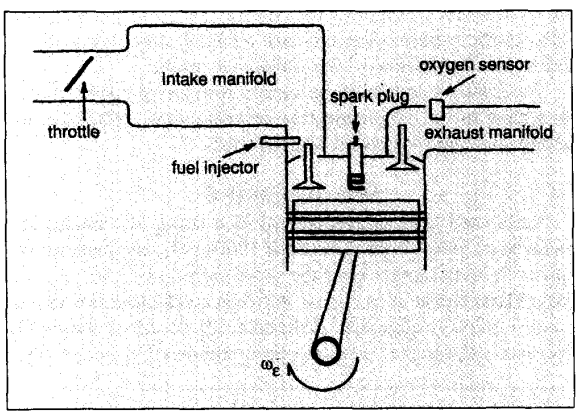

Fig. 3b. Engine model.

- the torque converter is locked
- the wheel slip is negligible
- the drive shaft is rigid

We can then formulate a five-state model which includes the throttle angle position, the intake manifold dynamics, the engine rotational speed, the vehicle longitudinal position, and the brake torque applied at the wheel. The mass continuity equation for the intake manifold is:

$$\dot{m}_a = \dot{m}_{a_i} - \dot{m}_{a_o} . \tag{1}$$

The mass of air flow rate through the throttle is:

$$\dot{m}_{a_i} = k_1 TC(\alpha) f_1(P_M) . \tag{2}$$

The ideal gas law in the intake manifold is:

$$P_m = \frac{RT_m}{M_{air} V_m} \cdot m_a . \tag{3}$$

The mass of air flow rate into the cylinder is:

$$\dot{m}_{a_o} = f_2(m_a, \omega_e) . \tag{4}$$

$\dot{m}_{a_i}$ is the mass rate of air flow through the throttle and is the product of a constant, k_1, related to the geometry of the manifold, an invertible throttle characteristic ($TC(\alpha)$) and a nonlinear function of the pressure ratio of the pressure in the manifold to atmospheric pressure due to the choked flow nature of the flow ($f_1(P_m)$). Equation (3) is an ideal gas law approximation that relates the pressure in the manifold (P_m) to the temperature in the manifold (T_m), the mass of air in the manifold (m_a) and M_{air} is the molecular weight of air. $\dot{m}_{a_o}$ is the airflow out of the intake manifold and into the cylinders and is a nonlinear function of the mass of air in the manifold and the engine RPM.

The rotational dynamics of the engine is given by:

$$J_e^* \dot{\omega}_e = T_{net}(\omega_e, P_m) - T_{load} , \tag{5}$$

where T_{net} is the net combustion torque, and J_e^* is an "effective engine inertia" which includes the engine, torque converter, drive shaft, tire and vehicle inertias, as well as the vehicle mass. T_{load} includes aerodynamic drag, brake torque, and rolling resistance terms, i.e.,

$$T_{load} = R_g^*(T_b + C_a R_g^{*2} h^3 \omega_e^2 + hF_r) , \tag{6}$$

where R_g^* depends on the gear ratio, T_b is the brake torque, C_a is the aerodynamic drag coefficient, h is the effective tire radius, and F_r is the rolling resistance at the wheels. It has been assumed in equation (6) that the vehicle speed and engine speed are related by:

$$v = hR_g^* \omega_e . \tag{7}$$

Throttle actuators, e.g., stepper motors, can be very fast, so assuming that the throttle angle, α, is a control variable is

reasonable. If a model that is affine in the control is desired, we can add a first-order model for the actuator dynamics, e.g., $\tau_t\dot{\alpha} + \alpha = \alpha_c$. Control of the brake torque, T_b, is not as straightforward and can be realized in several different ways, ranging from hydraulic actuation of the brake pedal, control of pressure at the master cylinder to individual brake actuators at each wheel. In this paper we will assume that a simple, linear first-order lag model is sufficient to show the general concepts[7], i.e.,

$$\tau\dot{T}_b + T_b = T_{b_c}\,, \tag{8}$$

where T_{b_c} is the commanded brake torque.

The dynamics of the intake manifold (Eq. (1)) are significantly faster than the engine speed (Eq. (5)) and brake torque (Eq. (8)) dynamics. Thus the approximation

$$\dot{m}_{a_i} \approx \dot{m}_{a_o} \tag{9}$$

would seem reasonable and would allow the net engine torque to be expressed directly as a function of the throttle angle, α, i.e.,

$$T_{net} = T_{net}(\alpha,\omega_e)\,. \tag{10}$$

Experiments conducted as part of the PATH program [18] have shown that inclusion of the intake manifold dynamics in the control system design significantly improves the vehicle following performance. We postulate that this is true because of unmodeled transport delays in the system.

Control Algorithm

Since the dynamic system is highly nonlinear and operates over a wide range, we sought a nonlinear control approach. References [2,16,18,19,20] describe the nonlinear control approach taken in the PATH longitudinal control program. The approach taken is a smoothed form of sliding mode control that can be briefly described as follows: The nonlinear system dynamics are[8]

$$\dot{\underline{x}} = \underline{f}(x) + \underline{g}(x)\underline{u}\,,$$

$$\underline{y} = \underline{h}(\underline{x})\,, \tag{11}$$

where $\underline{x} \in R^n$, and $\underline{u}$ and $\underline{y} \in R^m$. Define the error vector, $e \in R^m$, as

$$\underline{e} = \underline{y} - \underline{y}_d(t) \tag{12}$$

We define an m-vector, $\underline{S}$,

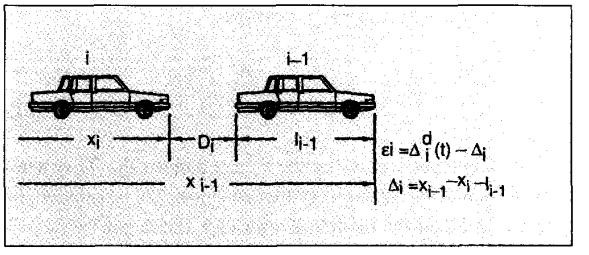

Fig. 4. Vehicle following nomenclature.

$$S_i \triangleq \left(\frac{d}{dt} + \lambda_i\right)^{r_i - 1} e_i\,,\ i \triangleq 1, m \tag{13}$$

where r_i is the relative degree of output y_i and $-\lambda_i$ is the desired closed-loop bandwidth. Differentiating (13) and using the definition of relative degree we can express $\dot{\underline{S}}$ as

$$\dot{\underline{S}} = \underline{l}(\underline{x}) + \underline{J}(\underline{x})\underline{u}\,. \tag{14}$$

Equation (14) will be affine in $\underline{u}$ as long as equation (11) is affine in $\underline{u}$ and $\underline{h}(\underline{x})$ has a well-defined relative degree for each scalar component. Under the assumption that $\underline{J}(\underline{x})$ is non-singular over the entire operating range we can define a "synthetic input,"

$$\underline{\mu} = \underline{l} + \underline{J}\,\underline{u} \tag{15}$$

such that

$$\underline{u} = \underline{J}^{-1}(\underline{\mu} - \underline{l}) \tag{16}$$

and

$$\dot{\underline{S}} = \underline{\mu}\,.$$

A convenient choice of $\underline{\mu}$ is

$$\underline{\mu} = -\underline{\Lambda}\underline{S}\,, \tag{17}$$

where $\underline{\Lambda}$ is a diagonal matrix such that

$$\dot{S}_i = -\lambda_i S_i\,. \tag{18}$$

This approach is convenient when dealing with modeling errors, e.g., if

$$\underline{f} = \underline{f}_m + \Delta\underline{f} \tag{19}$$

where $\underline{f}_m$ is the nominal model and $\underline{\Delta}$ represents the uncertainty. In this case (16) and (17) would not lead exactly to (18) but if we have knowledge of the modeling error bounds, we can choose the λ_i such that

$$S_i\dot{S}_i \le -\frac{\eta_i S_i^2}{\Phi_i}\,,\ \text{for}\ |S_i| \ge \Phi_i\,. \tag{20}$$

[7] In practice there will also be a pure time delay between the applied actuator voltage and the brake torque measured at the wheel. This effect is not considered here.

[8] In order to place equations (1)-(8) in the form of equation (11), i.e., affine in the control, we need to add a linear first-order model for the throttle actuator similar to the brake actuator model (8). The states would then be α, m_a, ω_e, T_b, and x_i (vehicle position), the controls would be throttle actuator voltage, α_c, and brake actuator voltage, T_b.

Condition (20) is sufficient to show that

$$\lim_{t\to\infty} | e_i | \leq \frac{\Phi_i}{\lambda_i^{r_i}} . \tag{21}$$

The design parameters are the λ_i in equation (18). They need to be chosen "large enough" so that equation (20) is satisfied. In general the larger the modeling error (Δf), the larger the λ_i will need to be. Slotine and Li [22] present a detailed treatment of this design methodology. This control structure also has advantages for nonlinear adaptive control [22].

If we apply this methodology to automated vehicle following we need the definitions defined in Fig. 4. We define the spacing error as:

$$\varepsilon_i = \Delta_i^d(t) - \Delta_i , \tag{22}$$

where $\Delta_i^d(t)$ is the desired spacing and Δ_i is the actual distance between vehicles. We next define a function of the vehicle spacing error that we would like to make equal to zero[9],

$$S_1 = \dot{\varepsilon}_i + q_1\varepsilon_i + q_2 \int_0^t \varepsilon_i d\tau . \tag{23}$$

Differentiating equation (23) and presuming that we would like S_1 to approach zero so that ε_i will approach zero, we set

$$\dot{S}_1 = -\lambda_1 S_1 . \tag{24}$$

In equation (24) we have assumed that if $\Delta f = 0$, if $\Delta f \neq 0$, then q_1, q_2, and λ_1 must be chosen such that an inequality in the form of equation (20) is satisfied. Equations (24) and (7) lead to:

$$\dot{\omega}_{e_d} = \frac{a_{i-1} - q_1\dot{\varepsilon}_i - q_2\varepsilon_i - \lambda_1 S_1}{R_g h} . \tag{25}$$

Equation (25) represents the desired angular acceleration of the engine. Equations (25), (5), and (6) lead to

$$T_{net_d} = J_e^*\dot{\omega}_{e_d} + R_g^* (T_b + C_a R_g^* h^3 \omega_e^2 + hF_r) . \tag{26}$$

Knowing the current ω_e we can use the steady-state engine maps ($T_{net}(\omega_e, m_a)$) to define a desired mass of air in the intake manifold, m_{a_d}. Since m_a is not a control we use the Multiple Sliding Surface method [23,24]

$$S_2 \stackrel{\Delta}{=} -m_a - m_{a_d} . \tag{27}$$

Differentiating and setting

$$\dot{S}_2 = -\lambda_2 S_2 \tag{28}$$

leads to

$$TC(\alpha) = (\dot{m}_{ao} + \dot{m}_{a_d} - \lambda_2 S_2)/k_1 f_1(P_m) . \tag{29}$$

The commanded throttle angle is obtained by inverting the throttle characteristic, $TC(\alpha)$. If the computed throttle angle is negative, then engine braking is not sufficient and a desired brake torque can be computed from equations (5) and (6), i.e.,

$$T_{b_d} = \frac{T_{net} - hR_g^*(C_a R_g^{*2} h^2 \omega_e^2 + F_r) - J_e^*\dot{\omega}_{e_d}}{R_g^*} . \tag{30}$$

Since T_b is not a control we define an additional surface

$$S_3 \stackrel{\Delta}{=} T_b - T_{b_d} . \tag{31}$$

Differentiating, using equation (8) and setting $\dot{S}_3 = -\lambda_3 S_3$ yields

$$T_{b_c} = \tau_b(\dot{T}_{b_d} - \lambda_3 S_3) + T_b . \tag{32}$$

In equations (22)-(32) the states and vehicle parameters are associated with the i^{th} vehicle.

The subject of combined throttle/brake control is currently being studied [25]. Unmodeled time delays and lags can lead to rapid switching between the throttle and brake. Introducing some hysteresis in the switching logic reduces the chattering but also increases the tracking error.

String Stability

The control laws (29) and (32) guarantee spacing error stability, i.e., assuming a perfect model we have $\lim_{t\to\infty}\varepsilon_i(t) \to 0$. Since we are forming a platoon of vehicles we need to be concerned about how disturbances at the front of the platoon propagate upstream to vehicles further down the platoon. This problem has been studied over the years [26,27,28] and leads to consideration of inter-vehicle communication requirements.

If we assume that we have a perfect model and if we neglect the intake manifold dynamics and the brake torque dynamics, i.e., we have instantaneous control of T_{net} and T_b, we can then eliminate all the nonlinearities[10] and directly control each vehicle's acceleration, i.e.,

$$\dot{v}_i = u_i . \tag{33}$$

The spacing error between the i^{th} and $i-1^{th}$ vehicle becomes:

$$\dot{\varepsilon}_i = v_i - v_{i-1} ,$$

[9]This is a modification of equation (13) since we have added an integral term, q_1 and q_2 are design parameters that must be positive to ensure the stability of $S_1 \equiv 0$.

[10]Clearly this is an ideal assumption. Simulations assuming reasonable model errors have validated the qualitative conclusions reached in this section.

$$\ddot{\varepsilon}_i = u_i - a_{i-1} \,. \tag{34}$$

References [26,27,28] study various control algorithms and their effect on string stability. Since we have linearized the system through our control we can use transfer function analysis to investigate string stability. In particular, we are interested in

$$\frac{\hat{\varepsilon}_i(s)}{\hat{\varepsilon}_{i-1}(s)} \stackrel{\Delta}{=} \hat{h}(s) \,, \tag{35}$$

where $\hat{\varepsilon}(s)$ is the Laplace transform of $\varepsilon(t)$. A well-known result from linear system theory is:

$$\| \varepsilon_i(t) \|_\infty \leq \| h(t) \|_1 \cdot \| \varepsilon_{i-1}(t) \|_\infty \,, \tag{36}$$

where the norms in equation (36) are defined for a function f(t),

$$\| (f(t)) \|_\infty \stackrel{\Delta}{=} \sup_{t \geq 0} | (f(t)) |$$

and

$$\| (f(t)) \|_1 \stackrel{\Delta}{=} \int_0^\infty | (f(\tau)) | \, d\tau \,.$$

A sufficient condition that guarantees disturbances will not amplify as they propagate upstream in the platoon is

$$\| h(t) \|_1 \leq 1 \,. \tag{37}$$

It is also well known from linear system theory [27] that

$$\| h(t) \|_1 \geq | \hat{h}(j\omega) | \,, \omega \geq 0 \,. \tag{38}$$

Thus a sufficient condition for string stability using equations (36), (37) and (38) is[11]

$$| \hat{h}(j\omega) | \leq 1 \,, \supset \omega$$

If the control in (33) is chosen by the smooth sliding control formulation, i.e.,

$$S_1 \stackrel{\Delta}{=} \dot{\varepsilon}_i + q_1 \varepsilon_i \,, \tag{39}$$

choose u_i such that

$$\dot{S}_1 = -\lambda S_1 \,, \tag{40}$$

then,

$$u_i = a_{i-1} - q_1 \dot{\varepsilon}_i - \lambda S_1 \,. \tag{41}$$

[11]This assumes that h(t) does not change sign.

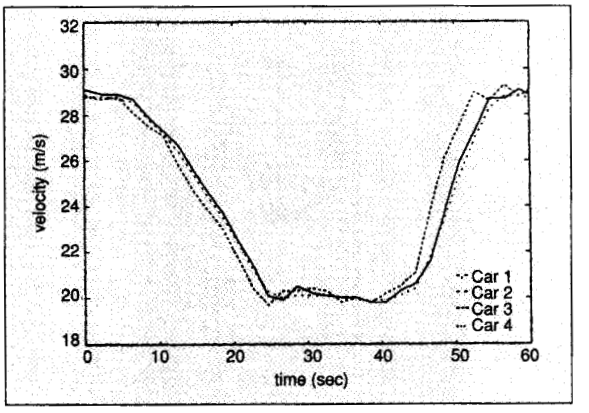

Fig. 5a. Four-car platoon velocities: Variable velocity profile.

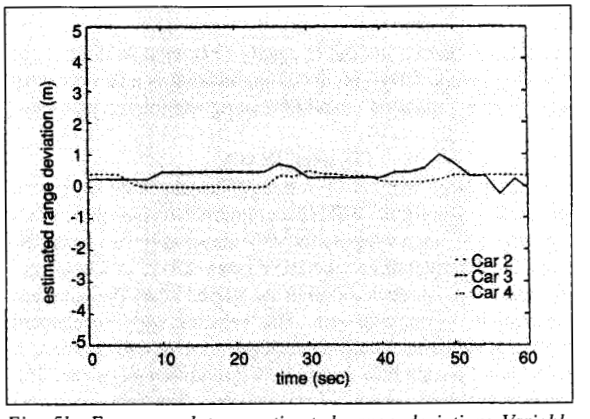

Fig. 5b. Four-car platoon estimated range deviation: Variable velocity profile.

This control law requires the knowledge of the acceleration of the preceding vehicle and completely decouples the dynamics of all vehicles so that (37) is satisfied. However, Ref. [28] showed that (41) is not robust to any modeling errors, e.g., if we approximate the control processing delay as

$$\tau \dot{u}_i + u_i = u_{i_d} \,. \tag{42}$$

Then it is straightforward to show that (37) is not satisfied and thus there exist disturbances which will amplify upstream. It is shown in Ref. [28] that redefining (39) to be

$$S_1 = \dot{\varepsilon}_i + q_1 \varepsilon_i + q_2 \, (v_i - v_l \, (t)) \,, \tag{43}$$

where v_l is the velocity of the lead vehicle in the platoon, and choosing u_i such that $\dot{S}_1 = -\lambda S_1$ leads to

$$u_i = \frac{1}{1 + q_2} [a_{i-1} + q_2 a_l \, (t) - (\lambda + q_1) \dot{\varepsilon}_i - \lambda q \varepsilon_i - \lambda q_2 (v_i - v_l \, (t))] \,. \tag{44}$$

This control law requires the acceleration of the preceding vehicle and the velocity and acceleration of the lead vehicle in the platoon. This control law increases the communication require-

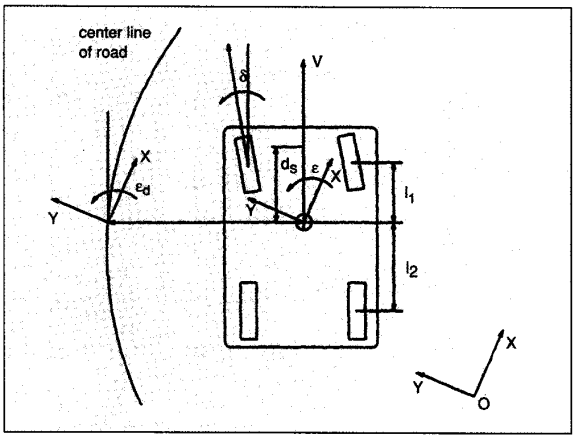

Fig. 6. Schematic diagram of linear vehicle model.

ments but is shown in [28] to satisfy (37) even in the case of modeling errors. Intervehicle communication is also necessary for emergency maneuvers and for exiting and joining platoons.

Field Test Results

A fairly large number of vehicle-following tests have been conducted as part of the PATH program over the past three years [29]. Fig. 5a,b shows results for variable speed tests conducted with a four-car platoon on the HOV lanes of I-15 in San Diego. The tests were conducted during the period when the lanes are unoccupied by other drivers. The vehicles were accelerated under manual control until a specified velocity was attained, at which point the throttle was switched to automatic mode. The driver maintained control of the steering. The first car in the platoon was accelerated and decelerated manually, while the following three vehicles were under automatic control. The vehicle following accuracy is seen to be quite good. The nominal spacing[12] was nine meters, with a following accuracy of ±1 meter.

Lateral Control

The vehicle lateral control system for AHS has two major functions: 1) lane following and 2) lane change maneuvering. Other important considerations include emergency handling and collision avoidance. In lane following, the control objectives are 1) to steer the wheels so that the vehicle tracks the center of a lane with a small error (e.g. cm) and 2) to maintain good ride quality under different vehicle speeds, loads, wind gust disturbances, and road surface conditions. Automated lane following was studied from the early 1960s [30-36]. Cardew [31] reported a position accuracy of ± 2cm on a straight test track in 1970. Another notable effort on lateral control in the 1970s was led by Fenton [33, 34]. Utilization of information related to the upcoming road characteristics is an important factor in the vehicle lateral control both in human driving and automated steering [37, 38]. PATH has examined several lateral control algorithms, including one based on the finite time preview control theory and the frequency shaped linear quadratic (FSLQ) control [38], one based on fuzzy rule-based control [39] and the other based on feedback linearization and surface control [40].

A vehicle lateral control system includes two major subsystems: a road reference/sensing system, which measures the position and orientation of the vehicle relative to the road, and an automated steering system aboard the vehicle. The latter consists of onboard sensors such as lateral accelerometers and a yaw-rate sensor, a control unit and a steering actuator. Various reference/sensing systems have been proposed in the past. Perhaps the oldest among them are wire reference schemes [30-34]. Other schemes include an optical marker system, an optical line-following system, various radar- and vision-based systems, a side-looking radar system with a reference side wall, and magnetic marker schemes. For a brief review of reference/sensing systems, see Fenton and Mayhan [41]. Guidance by permanently magnetized markers was studied in the early 1970s [42]. In this scheme, vehicle lateral displacement is obtained from the magnetic field strength intermittently. This scheme was revived in the late 1980s by Zhang, who proposed a robust signal processing scheme for obtaining the lateral error [43]. This system can provide not only the lateral tracking error to the control computer aboard the vehicle, but also other information such as preview road curvature information in binary form by alternating the polarity of the magnets. Furthermore, it compares favorably with other schemes in terms of evaluation criteria such as accuracy, reliability, maintainability, and cost. Therefore, the scheme has been adopted as the primary reference system in PATH.

In contrast to lane following, considerably less research has been conducted for the lane change maneuver problem. Godthelp [44] investigated human driving patterns, and found that, during a lane change, the steering wheel angle of a vehicle resembles a sine function, and that the lane change maneuver may be divided into four phases according to the signs of steering angle and its time derivative. Hess and Modjtahezadeh [45] proposed a preview controller model of a human driver for a lane following and a lane change maneuver. A recent PATH work on lane change maneuver addresses 1) the determination of the trajectory for the vehicle to follow between two automated lanes and 2) control schemes for robust lane change maneuver based on onboard sensors [46].

Vehicle Lateral Model

Fig. 6 shows a schematic diagram of the linear vehicle model used to design the control laws. The system equation for the front-wheel-steered vehicle is

$$\frac{d}{dt}\begin{bmatrix} y_r \\ \dot{y}_r \\ \Delta\varepsilon \\ \Delta\dot{\varepsilon} \end{bmatrix} = \begin{bmatrix} 0 & 1 & 0 & 1 \\ 0 & \frac{A_1}{V} & -A_1 & \frac{A_2}{V} \\ 0 & 0 & 0 & 0 \\ 0 & \frac{A_3}{V} & -A_3 & \frac{A_4}{V} \end{bmatrix} \begin{bmatrix} y_r \\ \dot{y}_r \\ \Delta\varepsilon \\ \Delta\dot{\varepsilon} \end{bmatrix} + \begin{bmatrix} 0 \\ B_1 \\ 0 \\ B_2 \end{bmatrix} \delta + \begin{bmatrix} 0 \\ A_1 - V^2 \\ 0 \\ A_4 \end{bmatrix} \frac{1}{\rho}, \tag{45}$$

where y_r is the lateral distance between the vehicle c.g. and the center line of the road, $\Delta\varepsilon = \varepsilon - \varepsilon_d$, ε is the yaw angle of vehicle body, ε_d is the desired yaw angle set by the road, δ is the front

[12] Recent field tests were conducted at 4 m spacing and no technical difficulties are anticipated at smaller spacing.

wheel steering angle, ρ is the radius of curvature of the road, denotes the time differentiation, and the vehicle parameters, A_i's and B_i's are defined as follows:

$$A_1 = \frac{-2(C_{sf} + C_{sr})}{m}\ ;\ A_2 = \frac{2(C_{sr}l_2 - C_{sf}l_1)}{m}\ ;\ B_1 = \frac{2C_{sf}}{m},$$

$$A_3 = \frac{2(C_{sr}l_2 - C_{sf}l_1)}{I_z}\ ;\ A_4 = \frac{-2(C_{sf}l_1^2 + C_{sr}l_2^2)}{I_z}\ ;\ B_2 = \frac{2l_1C_{sf}}{I_z} \quad (46)$$

l_1 and l_2 are the distance from c.g. to the front axle and rear axle, respectively, and C_{sf} and C_{sr} are the cornering stiffness of the front tires and the rear tires, respectively. Tire cornering stiffness describes the tire-road interaction. The output y_s taken as the measurement of lateral deviation from a sensor located at a distance d_s ahead of the mass center, can be expressed as:

$$y_s(t) = y_r(t) + d_s(\varepsilon(t) - \varepsilon_d(t))\ . \quad (47)$$

Preview FSLQ Control for Lane Following

The frequency dependent performance index is

$$J = \frac{1}{2\pi}\int_{-\infty}^{\infty} [a^*(j\omega)\frac{q_a^2}{1+\lambda_a^2\omega^2}a(j\omega)$$

$$+ y_s^*(j\omega)\frac{q_y^2}{1+\lambda_y^2\omega^2}y_s(j\omega) + \Delta\dot{\varepsilon}^*(j\omega)\frac{q_{\dot{\varepsilon}}^2}{1+\lambda_{\dot{\varepsilon}}^2\omega^2}\Delta\dot{\varepsilon}(j\omega)$$

$$+ y_s^*(j\omega)\frac{q_i^2}{(j\omega)^2}y_s(j\omega) + \delta^*(j\omega)R\delta(j\omega)]d\omega\ , \quad (48)$$

where a is the difference between the lateral acceleration of the vehicle mass center and its desired value (V^2/ρ). The coefficients q_a and λ_a are chosen so that the first term of J represents the ride quality. The coefficients of the next three terms are chosen so that the controller reacts to the road curves but is less responsive to the high-frequency measurement noise. In minimizing this performance index, it is assumed that the disturbance term in the vehicle model, w(t) = (1/ρ(t)), is previewed with a preview time t_{la}: i.e., $\{w(t+\sigma) \mid 0 \le \sigma \le t_a\}$ is known at time t.

In solving the preview FSLQ problem, the following two points have to be taken into consideration.

1. The frequency dependent quadratic performance index introduces dynamic filters for placing proper frequency dependent weights on the state variables. In the present problem, four first order filters are required, and the order of the overall system is increased by four, i.e. letting x denote the original state vector, the augmented state vector is $x_e^T = [x^T, z_1, z_2, z_3, z_4]$, where z_i's are the state of the filters.

2. The minimization of the performance index requires the knowledge of the disturbance, i.e. the radius of curvature, from the present time to infinity. Finite preview information is not sufficient for the determination of optimal control. It was assumed that the disturbance decays beyond the preview segment exponentially.

The optimal preview control law can be expressed as

$$\delta_{opt}(t) = -K_{xe}x_e(t) + \int_0^{t_{la}} K_{w1}(l)w(t+l)dl + K_{w2}w(t+t_{la})\ , \quad (49)$$

where the first term represents the state feedback control term and the second and third represent the preview control term. The details of the optimal preview FSLQ control are given in Peng and Tomizuka (1991).

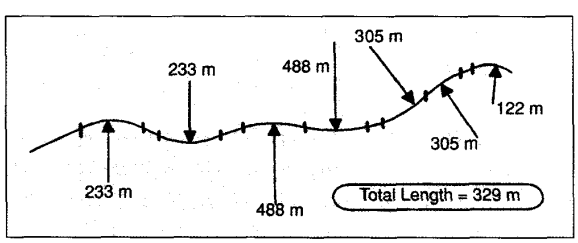

Fig. 7. Experimental track.

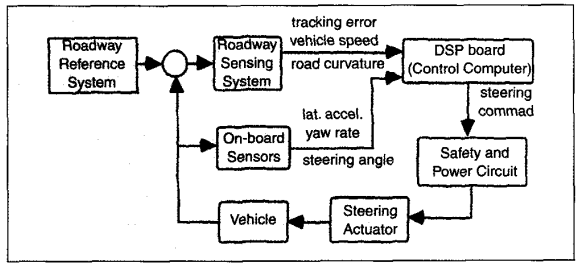

Fig. 8. Schematic diagram of the experimental setup.

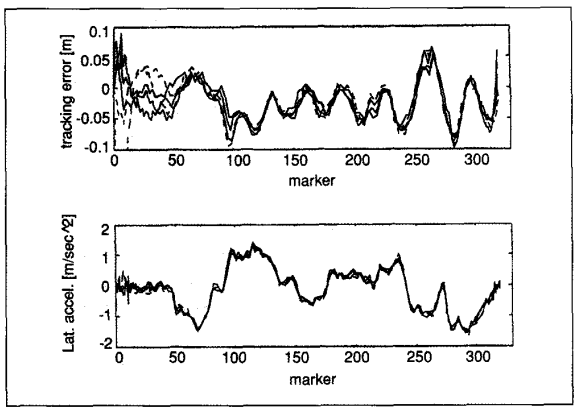

Fig. 9. Test results of FSLQ-preview control algorithm (50 km/hr).

Experimental Setup and Results

The optimal preview FSLQ control was evaluated by simulation and experiment for a variety of situations such as varying the preview time, vehicle speed, load, and road surface condition. Experimental setup and results are reviewed in this section. Two test tracks have been built at Richmond Field Station of the University of California. The details of the track used in experi-

ments presented in this paper are shown in Fig. 7. Magnetic markers are installed along the center of the test track at 1 m intervals. The road curvature information is encoded in the markers so that the vehicle controller has preview information 20 markers ahead. The schematic diagram of the PATH lateral control experimental system is shown in Fig. 8. Two magnetometers mounted beneath the middle of the front bumper measure the vertical and horizontal components of the magnetic field generated by each marker. These measurements are converted to the lateral error by the signal processing scheme outlined in [43]. Other sensors aboard the vehicle are a yaw rate sensor, a lateral accelerometer, and a steering angle sensor. The steering command from the control computer is a command in steering angle. A minor loop feedback controller for the steering actuator controls the front wheels to match the command.

PATH has conducted experiments on two test cars. The first experimental study used a Toyota Celica. More recently, the PATH is using a Pontiac 6000. The FSLQ control algorithm with preview has been successfully implemented on the two test vehicles. In fact, the software program required only very minor changes when it was transplanted from the Celica to the Pontiac test bed. The test results indicate that under nominal conditions, the vehicle under optimal preview FSLQ control is controlled within ±10 cm on the test track in Fig. 7. Fig. 9 shows the experimental results from five test runs. In this experiment, the stepping motor driven throttle is regulated by a PID controller to maintain the speed within a very small range about the command speed. While the longitudinal control is not a major emphasis and an error analysis has not been performed, the regulation error for the speed is about ±1 km/hr. It is our plan to implement the longitudinal controller from the previous section for combined longitudinal/lateral experiments. The vehicle failed to stay on the track without preview control. Details of the experiment are found in Peng, et al. (1992).

A series of tests for studying the robustness of the FSLQ control algorithm have been performed for the Toyota Celica. Robustness tests included 1) increased load, 2) reduced tire pressure, 3) missing magnetic markers and marker height variation, and 4) slippery road surface. While the tracking error and response speed were certainly affected under each perturbed condition, it was found that the controller was robust and reliable. The Toyota Celica was used for testing a fuzzy rule-based controller also [39].

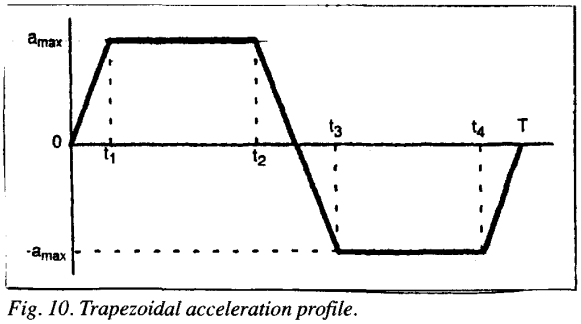

Fig. 10. Trapezoidal acceleration profile.

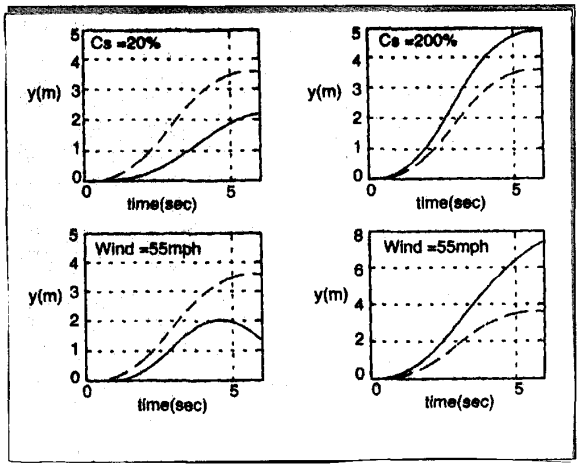

Fig. 11. Uncertainty analysis.

Lane Change Maneuver

The desired trajectory for a lane change maneuver is designed considering passenger's ride comfort and transition time. It is assumed that the distance between the centers of two adjacent lanes is d. Four candidate trajectories are 1) circular trajectory, which consists of two circular arcs with a curvature equal in magnitude but opposite in direction and a straight segment between the two arcs, 2) cosine trajectory, 3) 5th order polynomial trajectory, and 4) trapezoidal acceleration trajectory. They were evaluated using the transition time as a performance index, the lateral acceleration and jerk as constraints, and vehicle speed as a design parameter. The maximum allowable lateral acceleration and jerk were set 0.05 g and 0.1 g/s, respectively. These were somewhat conservative relative to 0.12 g and 0.24 g/s suggested by Caywood et al. [47]. The first two among the four candidate trajectories cannot satisfy the jerk constraint. However, the first is of value to set the standard for the transition time, and the second provides an easy parameterization of trajectories. Since the trapezoidal acceleration trajectory may be specified to satisfy both the acceleration and jerk constraints with a slight increase in the transition time as compared to the first, it was selected to be the optimal trajectory. A typical acceleration profile is shown in Fig. 10.

The transfer function of the linear model (45) from steering angle to y is written as

$$Y(s) = \frac{B_1 s^2 + \frac{B_2A_2 - B_1A_4}{V}s + B_1A_3 - B_2A_1}{s^2\left[s^2 - \frac{A_1 + A_4}{V}s + \frac{A_1A_4 - A_2A_3}{V^2} + A_3\right]}\Delta(s)\,, \tag{50}$$

where Y(s) and $\Delta(s)$ are the Laplace transforms of the lateral displacement and the steering angle, respectively, and ε_d and ρ have been set to 0 and ∞, respectively. The steering to force y(t) to remain the optimal desired trajectory is obtained by inverting this transfer function: i.e.,

$$\Delta(s) = \frac{s^2 - \frac{A_1 + A_4}{V}s + \frac{A_1A_4 - A_2A_3}{V^2} + A_3}{B_1s^2 + \frac{B_2A_2 - B_1A_4}{V}s + B_1A_3 - B_2A_1}\,[s^2Y_d(s)]\,. \tag{51}$$

$s^2Y_d(s)$ is the second derivative of $Y_d(s)$ and is in the trapezoidal form. Note that the parameters in the transfer function (50) depend on vehicle parameters as given by Eq. (46), and that the vehicle is subject to a wind disturbance, which does not appear in Eq. (45). Furthermore, Eq. (45) is a linearized model. Therefore, if the steering angle is adjusted according to Eq. (51) with nominal parameters, the actual lateral motion of the vehicle may be significantly different from the desired trajectory. Fig. 11 shows simulation results when the vehicle is given the steering input based on Eq. (51) with nominal parameters, C_s = 57,200 N/rad, m = 1,465 kg, I_z = 2,900 kg-m^2, l_1 = 1.12 m, l_2 = 1.41 m and V = 102 km/hour. As shown in the figure, the performance of vehicle is not acceptable. The performance can be improved by applying feedback control. The design of feedback controllers is currently under study. Some initial results are in [46]. At present, there is no agreement whether lane changes should be allowed only at specified places or randomly. Therefore, it is not practical to assume that reference trajectories are physically marked between two adjacent lanes, and the use of onboard sensors must be considered in the controller design.

Conclusions

Past and ongoing research in the California PATH program has shown that significant advances have been made in the technology leading up to an automated highway system. This paper has described preliminary control system architecture, vehicle following algorithms, and lane keeping algorithms. Computer simulations and field tests have proven the feasibility of the desired approach.

Current research is focusing on interactions between the various layers of the system architecture, as well as control problems associated with entry/exit, merging, and lane change maneuvers. In addition, continued investigations of alternative sensors and vehicle actuators are being conducted.

References

[1] R.G. Stefanek and D.F. Wilkie, "Control Aspects of a Dual-Mode Transportation System," *IEEE Trans. on Vehicular Technology*, vol. VT-22, no. 1, pp. 7-13, Feb. 1993.

[2] S.E. Shladover, et al., "Automatic Vehicle Control Developments in the PATH Program," *IEEE Trans. on Vehicular Technology*, vol. 40, no. 1, pp. 114-130, Feb. 1991.

[3] S.E. Shladover, "Potential Freeway Capacity Effects of Advanced Vehicle Control Systems," 2 Second International Conference on Applications of Advanced Technologies in Transportation Engineering, Minneapolis, Aug. 1991.

[4] P. Varaiya, "Smart Carts on Smart Roads: Problems of Control," *IEEE Trans. on AC*, vol. 38, no. 2, Feb. 1993.

[5] S. Sachs, D. Bodbole and P. Varaiya, "Entry and Exit Maneuvers," unpublished draft, March 17, 1994, EECS Dept., UC Berkeley.

[6] B.S.Y. Rao, P. Varaiya, and F. Eskafi, "Investigations into Achievable Capacity and Stream Stability with Coordinated Intelligent Vehicles," *Transportation Research Record*. To appear, 1993.

[7] A. Hitchcock, "Intelligent Vehicle/Highway System Safety: Multiple Collisions in AHS Systems." PATH Technical Report, Institute of Transportation Studies, University of California, Berkeley, Calif., 1994, to appear.

[8] J. Bender, "An Overview of Systems Studies of Automated Highway Systems," *IEEE Transactions on Vehicular Technology*, vol. 40, pp. 82-99, February 1991.

[9] B.S.Y. Rao and P. Varaiya, "Roadside Intelligence for Flow Control in an IVHS," *Transportation Research-C*, vol. 2, no. 1, pp. 49-72, 1994.

[10] A. Hsu, F. Eskafi, S. Sachs, and P. Varaiya, "Protocol Design for an Automated Highway System," *Discrete Event Dynamic Systems*, vol. 2, pp. 183-206, 1993.

[11] Z. Har'El and R.P. Kurshan, "Software for Analytical Development of Communications Protocols," *AT&T Technical Journal*, pp. 45-59, January/February 1990.

[12] F. Eskafi, D. Khorramabadi, and P. Varaiya, "SmartPath: An Automated Highway System Simulator," Tech. Rep., PATH Tech Memo 92-3, Institute of Transportation Studies, University of California, Berkeley, Calif. 94720, October 1992.

[13] W. S. Levine and M. Athans, "On the Optimal Regulation of a String of Moving Vehicles," *IEEE Trans. on AC*, vol. AC-11, no. 3, July 1966.

[14] A.S. Hauksdottir and R.E. Fenton, "On the Design of a Vehicle Longitudinal Controller," *IEEE Trans. Veh. Technol.*, vol. VT-34, pp. 182-187, Nov. 1985.

[15] S. Sheikholeslam and C.A. Desoer, "Longitudinal Control of a Platoon of Vehicles," *Proceedings of 1990 ACC, May 1990.*

[16] J.K. Hedrick, D. McMahon, V.K. Narendran, and D. Swaroop, "Longitudinal Vehicle Control Design for IVHS Systems," *Proceedings of 1991 ACC*, Boston, June 1991.

[17] D. Cho and J.K. Hedrick, "Automotive Powertrain Modeling for Control," *Trans. ASME, J. Dynamic Syst., Measur. and Contr.*, vol. 111, Dec. 1987.

[18] J.K. Hedrick, D.H. McMahon, and D. Swaroop, "Vehicle Modeling and Control for Automated Highway Systems," PATH Technical Report, UCB-ITS-PRR-93-24, 1993.

[19] J.J. Moskwa and J.K. Hedrick, "Nonlinear Algorithms for Automotive Engine Control," *IEEE Control Systems Magazine*, vol. 10, no. 2, pp. 88-93, April 1990.

[20] M. Tomizuka and J.K. Hedrick, "Automated Vehicle Control for IVHS Systems," 12th IFAC World Congress, Sydney, Australia, July 1993.

[21] B. Fernandez and J.K. Hedrick, "Control of Multivariable Nonlinear Systems by Sliding Modes," *International Journal of Control*, vol. 46, pp. 1019-1040, Sept. 1987.

[22] J.J. Slotine and W.P. Li, *Applied Nonlinear Control*, Prentice-Hall, 1991.

[23] J. Green and J.K. Hedrick, "Nonlinear Speed Control for Gasoline Engines," *Proceedings of the 1990 American Control Conference*, San Diego, May 1990.

[24] M.C. Won and J.K. Hedrick, "Multiple Sliding Surface Control for Nonlinear Systems," submitted to *International Journal of Control*, March 1994.

[25] J.C. Gerdes, et al., "Brake System Modeling for IVHS Longitudinal Control," *Advances in Robust and Nonlinear Control Systems*, 1993, DSC-vol. 53, ASME WAM, New Orleans, Nov. 1993.

[26] W.S. Levine and M. Athans, "On the Optimal Regulation of a String of Moving Vehicles," *IEEE Trans. AC*, vol. AC-11, no. 3, July 1966.

[27] C.A. Desoer and M. Vidyasagar, *Feedback Systems: Input-Output Properties*, Academic Press, N.Y., 1975.

[28] J.K. Hedrick and D. Swaroop, "Dynamic Coupling in Vehicles Under Automatic Control," *Proceedings of the 12th IAVSD Symposium*, Chengdu, China, August 1993.

[29] K.S. Chang et al., "Experimentation with a Vehicle Platoon Control System," *Proceedings of the 1991 Vehicle Navigation and Information Systems Conference*, Dearborn, Mich., Nov. 1991.

[30] K. Gardels, "Automatic Car Controls for Electronic Highways," General Motors Research Laboratory (GMR)-276), General Motors, Warren, Mich., June 1960.

[31] K.H.F. Cardew, "The Automatic Steering of Vehicles—An Experimental System Fitted to a DS19 Citroen Car," Road Research Laboratory (RRL) report LR340N, Great Britain.

[32] T. Ito, et al., "An Automatic Driving System of Automobiles by Guidance Cables," International Automotive Engineering Congress, SAE paper 730127.

[33] R.E. Fenton, et al., "On the Steering of Automated Vehicles: Theory and Experiment," *IEEE Transactions on Automatic Control*, vol. AC-21, no. 3, pp. 306-315, June 1976.

[34] R.E. Fenton and I. Selim, "On the Optimal Design of an Automotive Lateral Controller," *IEEE Trans. on Vehicular Technology*, vol. 37, no. 2, pp. 108-113, May 1988.

[35] J. Ackermann and W. Sienel, W., "Robust Control for Automatic Steering," *Proceedings of the American Control Conference*, pp. 795-800, 1990.

[36] H. Peng and M. Tomizuka, "Vehicle Lateral Control for Highway Automation," *Proceedings of American Control Conference*, pp. 788-794, 1990.

[37] A.Y. Lee, "Algorithm for Four-Wheel-Steering Passenger Vehicles," *Advanced Automotive Technologies*, 83-98, 1989.

[38] H. Peng and M. Tomizuka, "Preview Control for Vehicle Lateral Guidance in Highway Automation," *Proceedings of the 1991 American Control Conference*, 2621-2627, 1991. (Also *ASME Journal of Dynamic Systems, Meas. and Control*, vol. 115, pp. 679-686, Dec. 1993.)

[39] T. Hessburg and M. Tomizuka, "Fuzzy Logic Control for Lateral Vehicle Control," *Proceedings of IEEE Conf. on Control Applications '93*, Vancouver, 1993. (Also to appear in *Control Systems*.)

[40] H.A. Pham, J.K. Hedrick, and M. Tomizuka, "Combined Lateral and Longitudinal Control of Vehicles for Automated Highway Systems," *Proceedings of the 1994 American Control Conference*, Baltimore, Md., June 1994.

[41] R.E. Fenton and R.J. Mayhan, "Automated Highway Studies at the Ohio State University: An Overview," *IEEE Transactions on Vehicular Technology*, vol. 40, no. 1, pp. 100-113, February 1991.

[42] R. Mahrt, "Principles of Automatic Guidance of Vehicles on a Lane by Means of Permanent Magnet Nails and On-Board Computer Control," 21st Annual Conference of Vehicle Technology Group, IEEE, Washington DC, 1992.

[43] W. Zhang, et al., "An Intelligent Roadway Reference System for Vehicle Lateral Guidance/Control," *Proceedings of 1990 American Control Conference*, pp. 281-286, 1990.

[44] J. Godthelp, et al., "Open and Closed Loop Steering in a Lane Change Maneuver," *Institute for Perception: National Defense Research Organization TNO Group*, November 1983.

[45] R.A. Hess and A. Modjthaedzadeh, "A Preview Control Model of Driver Steering Behavior," *1989 IEEE International Conference on Systems, Man and Cybernetics.*

[46] W-S. Chee and M. Tomizuka, "Lane Change Maneuver of Automobiles for the Intelligent Vehicle and Highway System (IVHS)," *Proceedings of the 1994 American Control Conference.*

[47] W.C. Caywood, H.L. Donnely and N. Rubinstein, *Guideline for Ride-Quality Specifications Based on Transpo '72 Test Data*, Johns Hopkins University Applied Physics Laboratory, Washington, 1977 (available through the National Technical Information Service).

J. Karl Hedrick received his B.S. in engineering mechanics from the University of Michigan in 1966. He received his M.S. and Ph.D. in aeronautical and astronautical engineering from Stanford University in 1970 and 1971. He was a professor of mechanical engineering at Arizona State University from 1970-1973 and was professor of mechanical engineering at MIT from 1974-1988. In 1988 he joined the Department of Mechanical Engineering at the University of California at Berkeley, where he is now vice chair of graduate studies. He is currently editor of the *Vehicle System Dynamics Journal* and a fellow of ASME.

Masayoshi Tomizuka was born in Tokyo in 1946. He received his B.S. and M.S. degrees in mechanical engineering from Keio University, Tokyo, in 1968 and 1970, respectively. He received his Ph.D. degree in mechanical engineering from the Massachusetts Institute of Technology, Cambridge, Mass., in 1974. He joined the Department of Mechanical Engineering at the University of California at Berkeley in 1974, where he is currently a professor. He served as vice chair of mechanical engineering at the University of California at Berkeley from 1988 to 1991.

Pravin Varaiya is James Fife Professor of Electrical Engineering and Computer Sciences at the University of California, Berkeley. He received his Ph.D. in electrical engineering from U.C. Berkeley. He is the author, with P.R. Kumar, of *Stochastic Systems: Estimation, Identification, and Adaptive Control* (Prentice-Hall: 1986) and editor, with A. Kurzhanski, of *Discrete Event Systems: Models and Applications, Lecture Notes in Information Sciences*, vol. 103, Springer, 1988. His areas of research and teaching are in transportation systems, communication networks, and power systems.